Joint optimisation for pedestrian, information and energy flows in emergency response systems with energy harvesting and energy sharing

Huibo Bi, *Member, IEEE*, Wen-Long Shang *, *Member, IEEE*, Yanyan Chen and Kezhi Wang, *Senior Member, IEEE*

***Abstract*—The rapid progress in informatisation and electrification in transportation has gradually transferred public transport junctions such as metro stations into the nexus of pedestrian flows, information flows, computation flows and energy flows. These smart environments that are efficient in handling large volume passenger flows in routine circumstances can become even more vulnerable during emergency situations and amplify the losses in lives and property owing to power outage triggered service degradation and destructive crowed behaviours. On the bright side, the increasingly abundant resources contained in smart environments have enlarged the optimisation space of an evacuation process, yet little research has concentrated on the joint optimal resource allocation between transportation infrastructures and pedestrians. Hence, in the paper, we propose a queueing network based resource allocation model to comprehensively optimise various types of resources during emergency evacuations. Experiments are conducted in a simulated metro station environment with realistic settings. The simulation results show that the proposed model can considerably improve the evacuation efficiency as well as the robustness of the emergency response system during emergency situations.**

***Keywords*—Emergency Management, Transportation Infrastructure System Optimisation, Resource Allocation, Energy harvesting, G-networks.**

I. Introduction

NOWADAYS, with the growing destructive power of disasters in populated areas as well as the advancement in information and communications technology (ICT), electrified emergency response systems (ERS) have gradually become a norm for large-scale public, commercial and residential buildings. Unfortunately, emergency events occurred in built environments tend to cause power failure, which can completely or partially malfunction the emergency response system and seriously degrade the quality of services (QoS) for evacuees. In fact, power failure itself is one of the most frequent emergency events and could induce various destructive crowd behaviours due to panic disorder. Although most ERS possess battery-based power supplies, the intensive communications and computations involved to provide desired emergency services for evacuees could quickly drain the remaining energy of an ERS and result in injuries and fatalities. But like every coin has two sides, as the sheer concentration of evacuees and the sudden massive demands from their portable devices will exacerbate the burden of an ERS, they also bring various types of resources that can be utilised by the ERS to achieve better performance.

As can be seen from the system architecture in Figure 1, a typical ERS commonly consists of a sensing sub-system to collect environmental data, a decision-making sub-system to calculate emergency instructions, a notification sub-system to display emergency instructions, and a communication sub-system to maintain the information exchanges within the ERS. Among these components, the decision-making sub-system was not a mandatory requirement for old-fashioned ERS which only disseminate emergency messages among evacuees for alerting purpose. The main trending in the development of ERS is twofold: (1) in the front-end of ERS, with the prosperous of Internet of Things (IoT) applications [1], [2], resources from various IoT devices are inclined to be integrated and re-allocated for emergency sensing, communications and computations; (2) in the back-end of ERS, the design and proposal of more and more complex and elaborated emergency management algorithms for different emergency entities has led to the continuous evolution in the system architecture of ERS, from pure wireless sensor network (WSN) based ERS, WSN and cloud computing integrated ERS, WSN and mobile cloud computing integrated ERS, eventually to Internet of Things (IoT) and mobile cloud computing integrated ERS [3]. Owing to these on-going changes, the on-site IoT devices become the most vulnerable part of an ERS for two reasons: (1) they suffer from energy issues because of the limited battery capacity and the convergence of massive sensory and information flows; (2) they are directly exposed to hazards when emergency events break out.

Although reliability of energy supply has a considerable impact on the performance of ERS due to the use of on-site energy-restrained devices to emergency sensing, communications and computations, most of the previous research has been conducted under the assumption that ERS will fully function during the evacuation process. This can be impractical in many situations, especially with the increasing use of energy hungry IoT devices. The efforts to improve the resilience of energy supply of an ERS can be divided into two directions: the first

Huibo Bi, Wen-Long Shang and Yanyan Chen are with the College of Metropolitan Transportation, Beijing University of Technology, Beijing 100124, China P.R. E-mail: {huibobi, shangwl_imperial, cdyan}@bjut.edu.cn.

Keizhi Wang is with the Department of Computer and Information Sciences, Northumbria University, Newcastle upon Tyne NE1 8ST, UK. E-mail: kezhi.wang@northumbria.ac.uk.

* Corresponding author: Wen-Long Shang.

Manuscript received April 19, 2005; revised January 11, 2007.

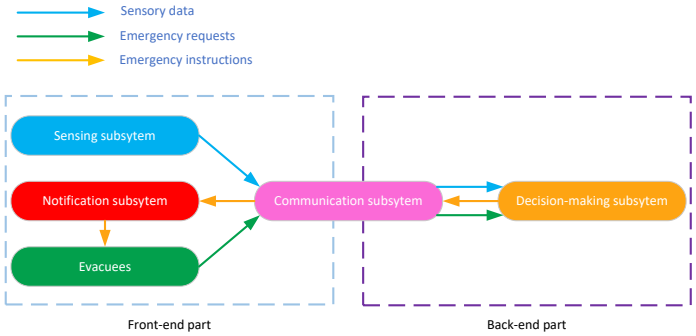

Fig. 1. System architecture of a typical emergency response system.

one is to develop various energy saving strategies to reduce the energy use in the system or energy balancing strategies to prolong the lifetime of devices; the second direction is to employ energy replenishment (ER) techniques to increase the energy supply in the system. Since the front-end of an ERS is normally formed by a wireless sensor network (WSN) or an IoT network, the former direction has been widely studied by researchers from wireless communications aspects [4], [5] and most of the contributions can be extended and applied to ERS. From network architecture aspect, heterogeneous network deployment algorithms [6] and various clustering techniques [7] have been proposed to satisfy the unbalanced energy usage in the network and prolong the network life time. From communication model aspect, various energy consumption models [8] and transmission mode adaptation algorithms [9] have been presented to precisely quantify the energy usage and dynamically adjust the transmission power to save energy in a single-device manner. From resource allocation aspect, enormous power-down schemes [10] and cooperative scheduling algorithms [11] have been presented to reduce energy consumption in a multiple-device manner. From routing pattern aspect, various static or mobile multi-path routing algorithms that consider differentiated QoS [12], [13] and relay/delay-tolerant strategies [14], [15] have been developed to achieve network level energy efficiency.

Although with various energy efficiency techniques [16], battery life is still the leading constraint for battery-operated devices owing to the current limited capacity of batteries. Thus, energy harvesting (EH) techniques have rapidly become a promising research domain in WSNs and IoT, and drawn considerable attention in the last decade. Energy sources including light, heat, motion and electromagnetic radiation are investigated and integrated into smart city IoT applications [17], such as wireless sensing systems [18], wireless monitoring systems [19], body sensor networks [20], wireless communications systems [21]. Apart from EH aided systems, other energy replenishment techniques have also been proposed to balance the energy distribution in the system such as mobile charger aided EH IoT networks [22], power over Ethernet (PoE) aided building management systems [23], wireless energy transfer aided smartphone chargers [24] and electric vehicle aided energy storage systems [25].

Owing to the significant energy dissipated in transportation [26], various ER algorithms and designs have been proposed in transportation systems [27]. For instance, the work in [28] employs kinetic energy harvesters to detect transportation mode for individuals. An electromagnetic energy harvester is designed to power a railway-WSN by harvesting vibration-induced energy of the track system [29]. Similar applications have been proposed to convert the deformation and vibration caused by vehicles [30] or pedestrians [31] into electrical energy via piezoelectric energy harvesters. Various regenerative braking systems have also been proposed to harvest the braking energy dissipated by trains [32] or vehicles [33]. Although with abundant algorithms and techniques for energy saving and energy replenishing, there are still lack of comprehensive models for the sufficient use of energy in a transportation system during emergency.

Hence, in this paper, we propose an energy management strategy with the aid of a queueing network model to optimise the energy assignment for on-site IoT devices during an evacuation process in a transportation junction. To maximise to life time of an ERS, we consider not only the remaining power of the system after the power is cut off, but also the possible energy harvested from various sources such as radio frequency, human movement, piezoelectric, etc. The queueing network model we employed is derived from a G-network model [34], which can mimic real world activities by introducing various entities and control factors with distinct capabilities and characteristics. By using this model, we optimise the energy assignment to each IoT device in the ERS with respect to movement of the evacuee traffic flows and emergency information flows. Specifically, the main contributions of this paper are summarized as follows.

1) We present a joint optimisation model for the optimisation of evacuee flows, information flows and energy flows in a resource limited emergency environment. The model can make sufficient use of the valuable resources within the hazardous area.
2) We present several accurate models to mimic the various interactive behaviours among pedestrians and various entities in transportation infrastructures in an evacuation process, including computation devices, energy storages, communication devices and actuation devices.
3) We propose a robust emergency management algorithm by leveraging the recent energy harvesting and energy sharing technologies. The proposed algorithm can considerably improve the service continuity under power outage conditions.

The remainder of the paper is organised as follows: we first review the related work in Section II, followed by problem formulation in Section III, which is composed of system description in III-A, and system approximation model in III-B. The solution approach to the problem is then presented in Section IV. The simulation models and results are introduced in Section V and VI, respectively. Finally, we draw conclusions in Section VII.

II. Related Work

Although much effort has been dedicated to energy efficient operations and energy harvesting in WSN or IoT based applications, to the best of the authors' knowledge, few have actually been implemented in ERS. Actually, most of the previous energy-efficient emergency management algorithms have concentrated on either communication aspect or computation aspect. The basic idea behind previous energy-efficient emergency management algorithms is to relay emergent messages or offload computations from low-energy devices to high-energy devices. For instance, the research in [35] utilises an *ad hoc* cognitive packet network (AHCPN) based routing protocol to search energy efficient and delay tolerant communication links for evacuees between portable devices and the back-end cloud center; packets are relayed to nearby portable devices with higher remaining power before performing energy-intensive uploading operations to the cloud center. Similarly, the work in [36] develops a smart cloud evacuation system to provide individual escape guidance with the aid of front-end smartphones and back-end datacenters; multimedia information such as text, voice and images gathered by smartphones are transmitted to datacenters for further human activity and emergency event analysis, so as to offload intense computations for saving energy at the front end. The study in [37] proposes a bio-inspired emergency alarm system to distribute emergency messages in an IoT network; a self-adaptive packet behaviour optimisation mechanism is proposed to reduce the energy consumption in communications and computations by dynamically adjusting parameters such as rate and time-to-live of data packets.

Since energy outage is one of the most common threats to physical entities during emergency, some research has been dedicated to the energy saving of vehicles, robots and electric wheelchairs. For instance, the study in [38] designs a cognitive packet network [39] based routing algorithm to search energy-efficient routes for disabled people in electric wheelchairs or mobile robots with respect to energy cost in typical motions like straight driving, turning and braking. The work in [40] proposes a G-network based control strategy to reduce the fuel consumption of vehicles during an large-scale evacuation by optimising the routing choices at intersections. Since people can lose their sense of direction and get trapped due to power failure or heavy smoke during a fire disaster, the research in [41] designs a novel emergency indicator that can harvest energy from water flows generated by automatic sprinklers and project holographic evacuation signs to highlight location of exits. The comprehensive optimisation of different resource flows in a built environment has also drawn growing attention in the recent years. For instance, the study in [42] proposes an edge-enabled emergency management framework to optimise the information flows and energy flows in public transportation junctions during an evacuation process; the movement directions of evacuees are also optimised for safety purpose but the possible harvesting of human kinetic energy is not taken into consideration. In summary, little research has applied energy efficient operations or EH technologies to ERS. In addition, although a substantial body of research has investigated the joint optimisation of data flows and energy flows [43], [44], little has considered the effect of evacuees' movement.

III. Problem Formulation

A. System Description

The target environment of our research can be a typical modernised transportation junction such as a metro station, but can be extended to other types of smart buildings. Generally, the transportation junction is assumed to possess an ERS composed of various IoT devices, including surveillance sensors (SSs), energy harvesting devices (EHDs), energy storages (ESs), computing devices (CDs), and actuation devices (ADs). SSs are employed to monitor the environmental situation [45], such as human motions, congestion level, disaster level, etc. The feasible sensors can be visual cameras for general purposes, or a combination of temperature sensors to detect hazard in fire related disasters, and Wi-Fi probes to count the number of evacuees in vicinity. EHDs are deployed at proper locations to gather environmental energy such as piezoelectric energy from human motions, radio frequency signals from portable devices. ESs such as batteries are utilised to deposit the incoming energy harvested from various energy sources, or energy transmitted from other energy storages. CDs are utilised to handle the local computations and data packet (jobs) sent from other computing devices. ADs such as lighting devices, portable devices, ventilation devices and alarming devices are used to conduct emergency response activities to defer the deterioration of the environment during emergency.

In our case, the designated system consists of scattered sensors to monitor the number of evacuees and hazard level of the immediate environment, piezoelectric harvesters to gather the mechanical energy of pedestrian flows, local computers to handle heavy computations, wireless energy transfers to gather the radiation energy transmitted from other IoT devices, batteries of IoT devices to store energy, and emergency lights to facilitate the evacuation process.

Specifically, we assume that evacuees are equipped with smart phones that can exchange information with nearby CDs. In reality, this can be implemented by installing a dedicated mobile application on the smart phones. We also assume that devices with pre-deployed wireless energy transfers can share energy with each others. When an evacuation starts, the ERS is activated and its constituent devices function as follows. SSs continuously collect sensory data including the hazard level, number of evacuees in vicinity and authorised personal information from smart phones in the immediate environment, and transmit the collected data to CDs. EHDs collect environmental energy and charge the ESs. ESs provide energy to SSs and wire-connected CDs, as well as charge other ESs under certain conditions. CDs periodically receive sensory data from SSs and generate emergency instructions based on the received sensory data. Since the means of generating emergency instructions (e.g. emergency routes) can be computationally intensive, and sensory data need to be shared among CDs for a better solution, a CD can send out data packets to offload tasks to other CDs and therefore form a cooperative computing pattern. When an evacuee with smart

phones approaches a SS, it can receive emergency messages from the SS and send personalised emergency requests to the CD via the SS. Evacuees can also provide energy to the ERS by passing through piezoelectric devices or to other evacuees via emitting radio frequency signals.

To manage and regulate the traffic flows, energy flows and information flows as shown in Figure 5, the ERS need to conduct several types of operations:

(1) SSs can perform bidirectional data transmission with CDs or other SSs in vicinity, which represents the process of sensory data collection and emergency instruction retrieval;
(2) SSs can perform bidirectional energy transmission with other SSs or portable devices in vicinity, which represents the process of wireless energy transferring;
(3) EHDs can perform unidirectional energy transmission to ESs in vicinity, which represents the process of energy harvesting;
(4) ESs can perform unidirectional energy transmission to wire-connected CDs, which represents the process of energy consuming during computations;
(5) ESs can perform bidirectional energy transmission with other connected ESs or portable devices, which represents the process of energy sharing;
(6) CDs can perform bidirectional data transmission with other CDs, which represents the process of information relaying;
(7) ESs can perform unidirectional energy transmission to ADs via portable devices or SSs, which represents the process of wireless energy transferring.

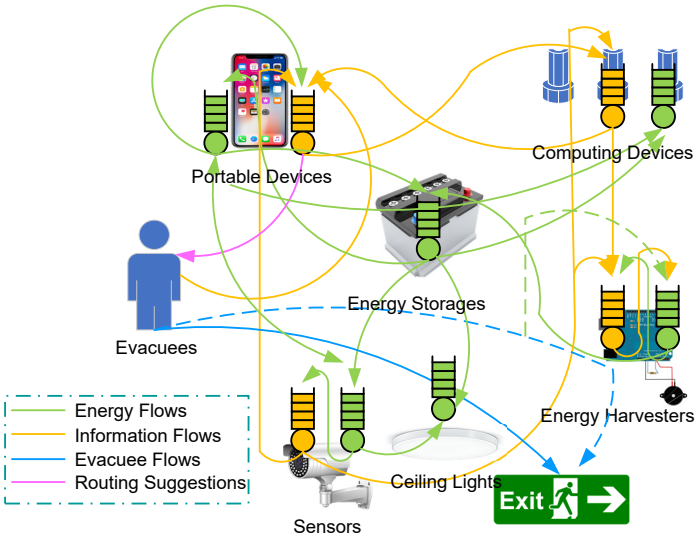

Fig. 2. The schematic representation of the various entity flows.

B. System Model

To model the operations and capture the dynamics of the aforementioned system, we utilise a G-network model with various types of entities to explicitly mimic the traffic flows, information flows and energy flows as well as the interactions among them. G-networks [46] are a class of queueing network models that can describe real-world processes and practical scenarios with basic entities —positive customers, and additional control factors including negative customers [47], removals [48], triggers [49] and resets [50]. G-networks have been used in a wide range of applications, including describing the workload in computer systems [51], [52], realising energy efficiency in packet networks [53], as well as modelling energy systems [54], [55], populations of biological agents [56] and gene regulatory networks [57]. One useful property of the G-networks is the existence of a product form solution (PFS) [49], where the joint equilibrium distribution of the number of positive customers in the network can be derived.

Specifically, the G-network model we used to describe the system is originated from [34], which contains various types of positive customers, negative customers and triggers. The nature and characteristics of these entities are described as follows:

- Positive customers: a positive customer of type k_p can enter a server v_i from the "outside world" with probability $\Lambda^+_{v_i,k_p}$ or from another server v_j inside the queueing network $N(v,e)$ and receive service at rate μ_{v_i} as ordinary queueing network customers. After service, they can either leave the network with probability L_{v_i,k_p} or move to another server v_j as a positive customer of type k'_p with probability $P^+_{(v_i,k_p),(v_j,k'_p)}$, as a negative customer of type k_n with probability $P^-_{(v_i,k_p),(v_j,k_n)}$ or a trigger of type k_t with probability $P^t_{(v_i,k_p),(v_j,k_t)}$.
- Negative customers: a negative customer of type k_n can enter a server v_i from the "outside world" with probability $\Lambda^-_{v_i,k_n}$ or from another server v_j inside the queueing network $N(v,e)$, it does not receive service and simply disappear when joined a server without positive customers. If a negative customer joins a non-empty server with positive customers, it will disappear after having destroyed a positive customer.
- Triggers: a trigger of type k_t can enter a server v_i from the "outside world" with probability $\Lambda^t_{v_i,k_t}$ or from another server v_j inside the queueing network $N(v,e)$, it also does not receive service and directly disappear when entered a server without positive customers. If it enters a non-empty server v_i with positive customers, it will disappear after having transfer a positive customer of type k_p to another linked server v_j as a positive customer of type k'_p with probability $Q_{(v_i,k_p),(v_j,k'_p)}$.

Specifically, for a positive customer of type k_p at server v_i, after being served, its transition probabilities satisfy the following condition:

$$L_{v_i,k_p} + \sum_{v_j=1}^{N_v} \sum_{k'_p=1}^{N^+_k} P^+_{(v_i,k_p),(v_j,k'_p)} + \sum_{v_j=1}^{N_v} \sum_{k_n=1}^{N^-_k} P^-_{(v_i,k_p),(v_j,k_n)} + \sum_{v_j=1}^{N_v} \sum_{k_t=1}^{N^t_k} P^t_{(v_i,k_p),(v_j,k_t)} = 1 \tag{1}$$

For a positive customer of type k_p at server v_i, after being triggered, its transition probabilities satisfies the following condition:

$$\sum_{v_j=1}^{N_v}\sum_{k'_p=1}^{N_k^+} Q_{(v_i,k_p),(v_j,k'_p)} = 1 \tag{2}$$

The probability that server v_i has one or more positive customers of type k_p can be derived from:

$$q_{v_i,k_p} = \frac{\lambda^a_{v_i,k_p}}{\mu_{v_i} + \lambda^s_{v_i,k_p}} \tag{3}$$

where $\lambda^a_{v_i,k_p}$ is the total arrival rate of positive customers of type k_p at server v_i, which includes the arrival of positive customers from the outside world, the arrival of positive customers from other servers after being served, and the arrival of positive customers from other servers after being triggered by internal-generated triggers, and the arrival of positive customers from other servers after being triggered by external arrival triggers:

$$\begin{aligned}\lambda^a_{v_i,k_p} = \Lambda^+_{v_i,k_p} &+ \sum_{v_j=1,v_j\neq v_i}^{N_v}\sum_{k'_p=1}^{N_k^+} q_{v_j,k'_p}\mu_{v_j} P^+_{(v_j,k'_p),(v_i,k_p)} \\ &+ \sum_{\substack{v_j=1,\\ v_j\neq v_i}}^{N_v}\sum_{k'_p=1}^{N_k^+} q_{v_j,k'_p}\mu_{v_j} \sum_{\substack{v_t=1,\\ v_t\neq\{v_j,v_i\}}}^{N_v}\sum_{k_t=1}^{N_k^t} P^t_{(v_j,k'_p),(v_t,k_t)} Q_{(v_t,k_t),(v_i,k_p)} \\ &+ \sum_{v_j=1,v_j\neq v_i}^{N_v}\sum_{k'_p=1}^{N_k^+} \Lambda^t_{v_j,k_t} q_{v_j,k'_p} Q_{(v_j,k'_p),(v_i,k_p)}\end{aligned} \tag{4}$$

On the other hand, $\lambda^s_{v_i,k_p}$ is the total departure rate of positive customers of type k_p at server v_i under the influence of signals, which includes the departure of positive customers after being removed by external or internal arriving negative customers, and the departure of positive customers to other servers after being triggered by external or internal arriving triggers:

$$\begin{aligned}\lambda^s_{v_i,k_p} = &\sum_{k_n=1}^{N_k^-} \Lambda^-_{v_i,k_n} + \\ &\sum_{v_j=1,v_j\neq v_i}^{N_v}\sum_{k_n=1}^{N_k^-} q_{v_j,k_n}\mu_{v_j} P^-_{(v_j,k_n),(v_i,k_p)} + \\ &\sum_{k_t=1}^{N_k^t} \Lambda^t_{v_i,k_t} + \\ &\sum_{v_j=1,v_j\neq v_i}^{N_v}\sum_{k_t=1}^{N_k^t} q_{v_j,k_n}\mu_{v_j} P^t_{(v_j,k_n),(v_i,k_p)}\end{aligned} \tag{5}$$

Based on the above model, we mimic the three key subsystems in the emergency response system, which are the evacuee navigation subsystem, information management subsystem, and power supply subsystem. Within the evacuee navigation subsystem: evacuees are treated as positive customers constantly before or after being served, reflecting the fact that evacuees will not change type or physical attributes after bypassing a PoI; PoIs where evacuees can congregate and change routes are modelled as "traffic" servers to serve evacuees; routing suggestions are modelled as triggers. When an emergency event breaks out, the interactive behaviours among evacuees and routing suggestions at PoIs are shown in Figure can be generally summarised as 4 types of actions by denoting the i-th PoI with n_i, the i-th type of evacuees with k^i_e and the i-th type of routing suggestions with k^i_d:

(1) initiate evacuation by leaving the origin PoI and starting to move towards the exits, this behaviour can be modelled in the G-network model by the external arrival of positive customers of type k^i_e at node n_i with a rate $\Lambda^+_{n_i,k^i_e}$;

(2) depart from one PoI to another PoI by sticking to their previous given evacuation routes, this behaviour can be modelled by the movement of "served" positive customers of type k^i_e from PoI n_i to another linked PoI n_j with probability $P^+_{(n_i,k^i_e),(n_j,k^i_e)}$ or being dropped at n_i with probability L_{n_i,k^i_e}, under the constraint that $L_{n_i,k^i_e} + \sum_{j=1}^{N}[P^+_{(n_i,k^i_e),(n_j,k^i_e)}] = 1$. Term L_{n_i,k^i_e} and $P^+_{(n_i,k^i_e),(n_j,k^i_e)}$ equals either 1 or 0 since all evacuees of a specific type only travel over a bench of deterministic routes at a given time. For instance, for a given evacuation route $\pi(n_1,n_2,n_e)$ for evacuees of type k^1_e from EN n_1 to EN n_e, we can describe it by setting $P^+_{(n_1,k^1_e),(n_2,k^1_e)} = 1$ and $P^+_{(n_2,k^1_e),(n_e,k^1_e)} = 1$. Since PoI n_e is an exit, term L_{n_e,k^i_e} is also set to 1 to describe the fact that EN n_e is the destination for all the packets traversing along the path;

(3) divert from one PoI to another PoI by following the newly arrived evacuation instructions, this behaviour can be modelled by the movement of positive customers of type k^i_e from node n_i to another linked PoI n_j with probability $Q_{(n_i,k^i_e),(n_j,k^i_e)}$ under the impact of arriving triggers at rate $\Lambda^t_{n_i,k^i_d}$, where $\sum_{j=1}^{N} Q_{(n_i,k^i_e),(n_j,k^i_e)} = 1$;

(4) complete evacuation by leaving the hazardous environment from the exits, this behaviour can be modelled by the movement of "served" positive customers of type k^i_e from exit n_e to the safe zone with probability $L_{n_e,k^i_e} = 1$.

As in the information management system, information packets are treated as positive customers before obtaining services. The processors in various IoT devices are modelled as "information" servers to serve information packets. Packet routing instructions are modelled as triggers, which can drive information packets to different destinations. After receiving services, information packets can either stay as positive customers or switch to signals to model various interactive behaviours: information packets can remain as positive customers to mimic an information transmission process, or change to triggers to mimic an information-triggered evacuee guidance process or an information-triggered energy relay process, or

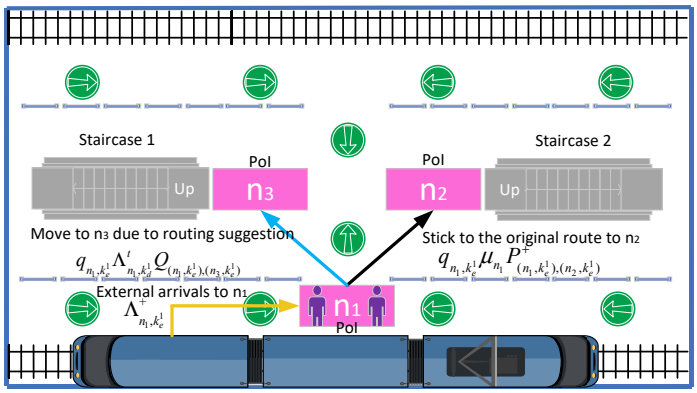

Fig. 3. The schematic representation of the evacuee navigation subsystem.

change to negative customers to mimic information-triggered computations, or in other words, the process of information packets being processed at the cost of some energy packets. Concretely, the information packets, including sensory data, emergency service requests, and emergency instructions, can conduct 7 types of behaviours during the evacuation process by denoting the i-th device with u_i, the i-th type of information packets k_d^i, and k_c^i, respectively:

(1) being generated at a device, this behaviour can be again mimicked in the G-network model by the external arrival of positive customers of type k_d^i at device u_i with a rate $\Lambda^+_{u_i,k_d^i}$;

(2) being transmitted from one device to another device and stay as information packets, this behaviour can be modelled by the movement of a "served" positive customer of type k_d^i from device u_i to another device u_j as a positive customer with probability $P^+_{(u_i,k_d^i),(u_j,k_d^i)}$;

(3) being transmitted from one device to another device and then trigger the computation process on device to generate emergency instructions, this behaviour can be modelled by the movement of a "served" positive customer of type k_d^i from device u_i to another device u_j as a trigger of type $k_d'^i$ with probability $P^t_{(u_i,k_d^i),(u_j,k_d'^i)}$;

(4) being relayed from one device to another device by following the newly arrived re-routing control instructions, this behaviour can be modelled by the movement of positive customers of type k_d^i from device u_i to another device u_j with probability $Q_{(u_i,k_d^i),(u_j,k_d^i)}$ under the impact of arriving triggers, where $\sum_{j=1}^{N} Q_{(u_i,k_d^i),(u_j,k_d^i)} = 1$;

(5) being transmitted from one device to another device and then trigger the computation process on device to consume a certain amount of energy, this behaviour can be modelled by the movement of a "served" positive customer of type k_d^i from device u_i to another device u_j as a negative customer of type $k_d''^i$ with probability $P^-_{(u_i,k_d^i),(u_j,k_d''^i)}$;

(6) being dropped due to time-out effect, this behaviour can be modelled by the destruction of a positive customer of type k_d^i at device u_i owing to the arrival of external negative customers with a rate of $\Lambda^-_{u_i,k_d^i}$.

(7) being deleted from one device after being used, this behaviour can be modelled by the movement of a "served" positive customer of type k_d^i leave the network from device u_i with a certain probability L_{u_i,k_d^i}.

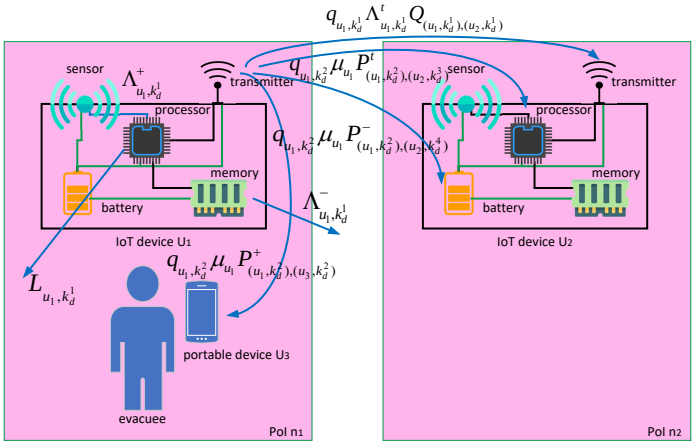

Fig. 4. The schematic representation of the information management subsystem.

In the power supply system, energy packets are considered as positive customers before obtaining services. The battery in IoT devices as well as ESs are modelled as "energy" servers to serve energy packets. Control instructions of the energy packets are treated as triggers. The standby losses or energy leakages of the IoT devices as well as ESs are modelled by the arrival of negative customers at non-zero servers. After receiving services, energy packets will always remain as positive customers and head towards another device to mimic an energy transmission process, or leave the network to model the energy consumption process. Concretely, the course of actions of energy packets during the evacuation process is described as follows by denoting i-th device or ES with u_i and the i-th category of energy packets k_c^i:

(1) being generated at a device, this behaviour can be again mimicked in the G-network model by the external arrival of positive customers of type k_c^i at device u_i with a rate $\Lambda^+_{u_i,k_c^i}$;

(2) being transmitted from one device to another device and stay as energy packets, this behaviour can be modelled by the movement of a "served" positive customer of type k_c^i from device u_i to another device u_j as a positive customer with probability $P^+_{(u_i,k_c^i),(u_j,k_c^i)}$;

(3) being relayed from one device to another device by following the newly arrived re-routing control instructions, this behaviour can be modelled by the movement of positive customers of type k_c^i from device u_i to another device u_j with probability $Q_{(u_i,k_c^i),(u_j,k_c^i)}$ under the impact of arriving triggers, where $\sum_{j=1}^{N} Q_{(u_i,k_c^i),(u_j,k_c^i)} = 1$;

(4) being consumed at a device owing to the computation process triggered by control instructions, this behaviour can be modelled by the movement of a "served" positive customer of type k_c^i leave the network from device u_i when being transmitted from device u_i to another device u_j with a certain probability L_{u_i,k_c^i}.

(5) being lost at a device due to standby losses or energy leakages, can be modelled by the destruction of a positive customer of type k_c^i at device u_i owing to the arrival of external negative customers with a rate of $\Lambda^-_{u_i,k_c^i}$

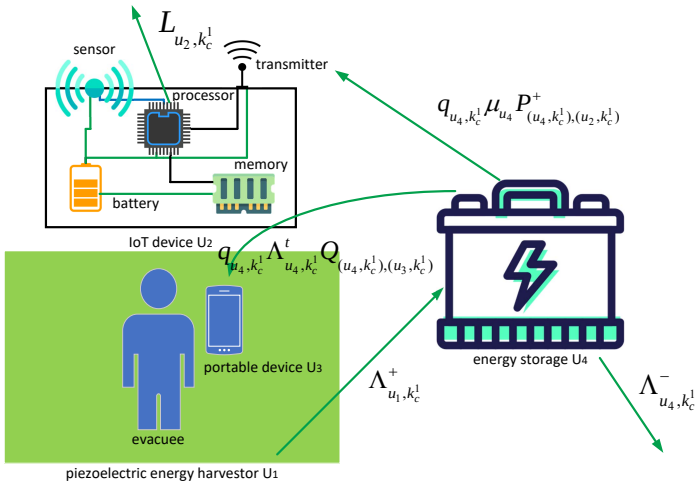

Fig. 5. The schematic representation of the power supply subsystem.

In summary, based on the aforementioned behaviour models of evacuees, information packets and energy packets, we generate 3 separate models to mimic the different behaviours in the system: in the evacuee navigation system, the external arrival/movement/exit of evacuees are modelled by the movement of positive customers, the arrival of evacuation instructions are modelled by the generation of external triggers, the interactive behaviours among evacuees and evacuation instructions are modelled by the interactions among positive customers and external triggers; in the information management system, the generation/transmission/loss of normal data packets are modelled by the movement of positive customers, the arrivals of packet routing instructions are modelled by the generation of external triggers, the processes of IoT devices making evacuation suggestions based on the arriving sensory data are modelled by the transformation of positive customers to triggers after being served, the energy consumed computation processes of IoT devices are modelled by the transformation of positive customers to negative customers after being served, the interactive behaviours among data packet and packet routing instructions are modelled by the interactions among positive customers and external triggers; in the power supply system, the generation/transmission/consumption of energy packets are modelled by the movement of positive customers, the arrivals of energy relay instructions are modelled by the generation of external triggers, the standby losses/energy leakages of IoT devices are modelled by the external arrivals of negative customers, the interactive behaviours among energy packet and energy relay instructions are modelled by the interactions among positive customers and external triggers.

IV. Solution Approach

To optimise the pedestrian flows, information flows and energy flows in a comprehensive manner, the key challenge is to bridge the gap among the evacuee navigation subsystem, the information management subsystem and the power supply subsystem. A straightforward approach is to use the "control packets" (which carry the control instructions) in the information management subsystem to establish the connections among the three subsystems. This is also realistic since the evacuation instructions for evacuees as well as the re-routing control instructions for information packets and energy packets are actually transmitted through the control packets in the information management subsystem.

For the evacuee navigation subsystem, the probability that a PoI n_i has one or more evacuees of class k_e^i can be derived from Equation (3):

$$q^{en}_{n_i,k_e^i} = \frac{\lambda^{a_{en}}_{n_i,k_e^i}}{\mu^{en}_{n_i} + \lambda^{s_{en}}_{n_i,k_e^i}} \tag{6}$$

where $\lambda^{a_{en}}_{n_i,k_e^i}$ is the total arrival rate of evacuee class k_e^i to PoI n_i, including evacuees that initially leave from n_i, and the evacuees that are arrived from other PoIs. Since the type of evacuees cannot change during the evacuation process, hence we can simplify Equation (4) as $\lambda^{a_{en}}_{n_i,k_e^i} = \Lambda^+_{n_i,k_e^i} + \sum_{n_j=1,n_j\neq n_i}^{N_{en}} q_{n_j,k_e^i}\mu^{en}_{n_j}P^+_{(n_j,k_e^i),(n_i,k_e^i)} + \sum_{n_j=1,n_j\neq n_i}^{N_{en}} \Lambda^t_{n_j,k_e^i}q_{n_j,k_e^i}Q_{(n_j,k_e^i),(n_i,k_e^i)}$. Term N_{en} stands for the number of PoIs inside the system. Term $\mu^{en}_{n_i}$ represents the service rate of PoI n_i to evacuee class k_e^i. Term $\lambda^{s_{en}}_{n_i,k_e^i}$ is the arrival rate of evacuation instructions at PoI n_i for evacuees of type k_e^i. Since we only have one type of evacuation instruction (navigation information) and we do not introduce "negative customers" in this model, hence we can simplify Equation (5) as $\lambda^{s_{en}}_{n_i,k_e^i} = \Lambda^t_{n_i,k_e^i}$. We also assume that there are N^c_{en} categories of evacuees in the subsystem, such as normal evacuees, elder evacuees, emergency personals.

For the information management subsystem, the information flows can be abstracted as "jobs". Since the key objective of the emergency response subsystem is to gather hazard information and generate emergency instructions for evacuees, hence we can describe the dynamics of information flows from the "sensory jobs" and "emergency instruction generation jobs" point of view. The probability that a device u_i has one or more emergency jobs of class k_d^i can be derived from Equation (3):

$$q^{im}_{u_i,k_d^i} = \frac{\lambda^{a_{im}}_{u_i,k_d^i}}{\mu^{im}_{u_i} + \lambda^{s_{im}}_{u_i,k_d^i}} \tag{7}$$

where $\lambda^{a_{im}}_{u_i,k_d^i}$ is the total arrival rate of emergency jobs of class k_d^i to device u_i, the jobs that are generated from the current device u_i can be represented by $\Lambda^+_{u_i,k_d^i}$, the jobs

that are processed by other devices and then transmitted to the current device for further processing (e.g. sensory jobs) can be described as $\sum_{u_j=1,u_j\neq u_i}^{N_{im}} q_{u_j,k_d^i}\mu_{u_j}^{im}P^+_{(u_j,k_d^i),(u_i,k_d^i)}$, the jobs that can not processed by other devices and are directly relayed to the current device (e.g. emergency instruction generation jobs) can be denoted by $\sum_{u_j=1,u_j\neq u_i}^{N_{im}} \Lambda^t_{u_j,k_d^i}q_{u_j,k_d^i}Q_{(u_j,k_d^i),(u_i,k_d^i)}$. Hence we have $\lambda^{a_{im}}_{u_i,k_d^i} = \Lambda^+_{u_i,k_d^i} + \sum_{u_j=1,u_j\neq u_i}^{N_{im}} q_{u_j,k_d^i}\mu_{u_j}^{im}P^+_{(u_j,k_d^i),(u_i,k_d^i)} + \sum_{u_j=1,u_j\neq u_i}^{N_{im}} \Lambda^t_{u_j,k_d^i}q_{u_j,k_d^i}Q_{(u_j,k_d^i),(u_i,k_d^i)}$. Term N_{im} stands for the number of IoT devices within the system. Term $\mu_{u_i}^{im}$ represents the service rate of device u_i to job class k_d^i. Term $\lambda^{s_{im}}_{u_i,k_d^i}$ is the operation rate of job re-dispatching instructions at device u_i for jobs of type k_d^i, including the jobs that are processed by this device and the jobs that are dropped owing to time-out effect, hence we have $\lambda^{s_{im}}_{u_i,k_d^i} = \Lambda^t_{u_i,k_d^i} + \Lambda^-_{u_i,k_d^i}$. We also assume that there are N_{im}^c categories of information packets in the subsystem, such as sensory data, emergency instructions, packet re-routing instructions.

For the power supply system, the energy flows can be described by "energy packet networks" [58], which use discrete units of energy to model the generation, store and consumption of energy systems. In general, energy can be generated by energy harvesters, stored by batteries, consumed by "jobs" and standby losses, and relayed to other devices or energy storages. The probability that a device u_i has one or more energy packets of class k_c^i can be again derived from Equation (3):

$$q^{ps}_{u_i,k_c^i} = \frac{\lambda^{a_{ps}}_{u_i,k_c^i}}{\mu^{ps}_{u_i} + \lambda^{s_{ps}}_{u_i,k_c^i}} \tag{8}$$

where $\lambda^{a_{ps}}_{u_i,k_c^i}$ is the total arrival rate of energy packets of class k_c^i to device u_i, the energy packets that are generated from the current device u_i can be represented by $\Lambda^+_{u_i,k_c^i}$, the constant energy flows that are transmitted from other devices (e.g. such as the internal transmission of energy from battery to processor on the same device) can be described as $\sum_{u_j=1,u_j\neq u_i}^{N_{ps}} q_{u_j,k_c^i}\mu_{u_j}^{ps}P^+_{(u_j,k_c^i),(u_i,k_c^i)}$, the random energy flows that that are transmitted from other devices (e.g. the energy transmissions among smartphones via wireless energy transfer) can be denoted by $\sum_{u_j=1,u_j\neq u_i}^{N_{ps}} \Lambda^t_{u_j,k_c^i}q_{u_j,k_c^i}Q_{(u_j,k_c^i),(u_i,k_c^i)}$. Hence we have $\lambda^{a_{ps}}_{u_i,k_c^i} = \Lambda^+_{u_i,k_c^i} + \sum_{u_j=1,u_j\neq u_i}^{N_{ps}} q_{u_j,k_c^i}\mu_{u_j}^{ps}P^+_{(u_j,k_c^i),(u_i,k_c^i)} + \sum_{u_j=1,u_j\neq u_i}^{N_{ps}} \Lambda^t_{u_j,k_c^i}q_{u_j,k_c^i}Q_{(u_j,k_c^i),(u_i,k_c^i)}$. Term N_{ps} stands for the total number of ES or battery of the IoT devices within the system. Term $\mu_{u_i}^{ps}$ represents the transmission rate of device u_i to energy packets class k_c^i. Term $\lambda^{s_{ps}}_{u_i,k_c^i}$ is the consumption rate for energy packets of type k_c^i at device u_i, including the energy packets that are relayed to other devices and the energy packets that are consumed by the standby losses, hence we have $\lambda^{s_{ps}}_{u_i,k_d^i} = \Lambda^t_{u_i,k_c^i} + \Lambda^-_{u_i,k_c^i}$. We also assume that there are N_{pc}^c categories of information packets in the subsystem, such as energy packet for computation jobs, energy packet for sensing jobs.

The probability that a general location (a PoI or a device) l_i has at least one entity (evacuees, information packets, and energy packets) is given by:

$$q_{l_i} = \sum_{j\in K} q_{l_i,k^j} \tag{9}$$

where term K stands for the number of types of entities. This probability q_{l_i} can be derived under the hypothesis that the average service rates μ_{l_i} of different types of entities at a given location are equal. This is reasonable because the average service rate of a location is mainly determined by the characteristics of the location. Since the entities are processed in a first-come-first-served order, and the average arrival rate of control instructions $\lambda^s_{l_i,k^i}$ are also equal, then we have $q_{l_i} = \frac{\sum_{j\in K}\lambda^a_{l_i,kj}}{\mu_{l_i}+\lambda^s_{l_i,k^j}} = \sum_{j\in K} q_{l_i,k^j}$.

Hence, the average number of entities (evacuees, information packets, and energy packets) at a general location l_i is given by:

$$N_{l_i} = \frac{q_{l_i}}{1-q_{l_i}} \tag{10}$$

In addition, by leveraging the product form solution (PFS) of G-networks, let $K^e_{l_i}(t)$, $K^d_{u_j}(t)$ and $K^c_{u_j}(t)$ denote the number of evacuees, information packets, and energy packets at time t at PoI n_i, IoT device u_j or battery u_m, respectively, we can obtain the joint probability distribution of number of entities:

$$\begin{aligned}&\Pr(K^e_{l_i}(t)=k_i^e,\ K^d_{u_j}(t)=k_j^d,\ K^c_{u_j}(t))=k_j^c,\\ &i=1,2,\ldots,N_n,\ j=1,2,\ldots,N_u)=\\ &\prod_{i=1}^{N_{en}} q_{n_i}^{k_i^e}(1-q_{n_i})\prod_{j=1}^{N_{im}} q_{u_j}^{k_j^d}(1-q_{u_j})\\ &\prod_{m=1}^{N_{ps}} q_{u_m}^{k_j^c}(1-q_{u_m})\end{aligned} \tag{11}$$

where term q_{n_i}, q_{u_j} and q_{u_m} stand for the utilization rate of evacuees, information packets, and energy packets, and can be obtained from Equation (9).

To jointly optimise the pedestrian flows, information flows and energy flows, we design a goal function contains the three confliction terms:

$$\begin{aligned}G = &\alpha\sum_{i=1}^{N_{en}}(N_{n_i}-O_{n_i})^2 + \beta\sum_{j=1}^{N_{im}}\frac{q_{u_j}}{\Lambda^+_{u_j}(1-q_{u_j})}\\ &+\gamma\sum_{m=1}^{N_{ps}} q_{u_m}^{N_{ps}(u_m)}\end{aligned} \tag{12}$$

where term α, β and γ are correlation coefficients that coordinate the relative importance between the three factors. Term O_{n_i} represents the optimal potential of the number of evacuees at PoI n_i, and can be derived by Equation (13). Term $\frac{q_{u_j}}{\Lambda^+_{u_j}(1-q_{u_j})}$ stands for the average service latency of the information and term $q_{u_m}^{N_{ps}(u_m)}$ represents the probability that

there are $N_{ps}(u_m)$ or more energy packets in the battery u_m, and $N_{ps}(u_m)$ is directly proportional to N_{n_i}.

$$O_{n_i} = N_e \frac{\frac{1}{Hz(n_i)}}{\sum_{i=1}^{N_n} \frac{1}{Hz(n_i)}} \tag{13}$$

where $Hz(n_i)$ stands for the hazard intensity and be can calculated by the product of hazard level and distance to the nearest exit of the current PoI.

The optimal solution of the goal function can be solved by the using gradient descent algorithm via selecting the desired flow ratios $Q_{(v_i,k_p),(v_j,k'_p)}$ for evacuees, information flows and energy flows. Please note that $\lambda^{a_{im}}_{u_i,k^i_d} = \Lambda^{-}_{u_i,k^i_c}$ as we assume that every job consumes an energy packet. To bridge the relation among the goal function (12) and an arbitrary probability choice $Q_{(v_x,k_m),(v_y,k_n)}$ at any node or device, we can utilise the chain rule as shown in Equation (14).

$$\frac{\partial G}{\partial Q_{(v_x,k_m),(v_y,k_n)}} = \alpha \sum_{i=1}^{N_{en}} \frac{\partial G}{\partial N_{n_i}} \frac{\partial N_{n_i}}{\partial q_{n_i}} \frac{\partial q_{n_i}}{\partial Q_{(v_x,k_m),(v_y,k_n)}} + \beta \sum_{j=1}^{N_{im}} \frac{\partial G}{\partial q_{u_j}} \frac{\partial q_{u_j}}{\partial Q_{(v_x,k_m),(v_y,k_n)}} + \gamma \sum_{m=1}^{N_{ps}} \frac{\partial G}{\partial q_{u_m}} \frac{\partial q_{u_m}}{\partial Q_{(v_x,k_m),(v_y,k_n)}} \tag{14}$$

The derivatives of goal function G with respect to N_{n_i}, q_{u_j} and q_{u_m} are:

$$\frac{\partial G}{\partial N_{n_i}} = \frac{1}{2}(N_{n_i} - O_{n_i}) \tag{15}$$

$$\frac{\partial G}{\partial q_{u_j}} = \frac{1}{\Lambda^{+}_{u_j}} \left[\frac{q_{u_j}}{(1-q_{u_j})^2} + \frac{1}{1-q_{u_j}} \right] \tag{16}$$

$$\frac{\partial G}{\partial q_{u_m}} = N_{ps}(u_m) q_{u_m}^{N_{ps}(u_m)-1} \tag{17}$$

The derivatives of N_{n_i} with respect to q_{n_i} is:

$$\frac{\partial N_{n_i}}{\partial q_{n_i}} = \frac{q_{n_i}}{(1-q_{n_i})^2} + \frac{1}{1-q_{n_i}} \tag{18}$$

The derivatives of q_{n_i}, q_{u_j} and q_{u_m} with respect to $Q_{(v_x,k_m),(v_y,k_n)}$ are:

$$\frac{\partial q_{n_i}}{\partial Q_{(v_x,k_m),(v_y,k_n)}} = \frac{1}{\mu^{en}_{n_i} + \Lambda^{t}_{n_i,k^i_e}} \sum_{j=1}^{N_{en}} \left\{ \Lambda^{t}_{n_i,k^i_e} q_{n_i} \frac{\partial Q_{(n_j,k^i_e),(n_i,k^i_e)}}{\partial Q_{(v_x,k_m),(v_y,k_n)}} + \left[\mu^{en}_{n_j} P^{+}_{(n_j,k^i_e),(n_i,k^i_e)} + \Lambda^{t}_{n_j,k^i_e} Q_{(n_j,k^i_e),(n_i,k^i_e)} \right] \frac{\partial q_{n_j}}{\partial Q_{(v_x,k_m),(v_y,k_n)}} \right\} \tag{19}$$

$$\frac{\partial q_{u_j}}{\partial Q_{(v_x,k_m),(v_y,k_n)}} = \frac{1}{\mu^{im}_{u_j} + \Lambda^{t}_{u_j,k^i_d} + \Lambda^{-}_{u_j,k^i_d}} * \sum_{i=1}^{N_{im}} \left\{ \Lambda^{t}_{u_i,k^i_d} q_{u_i} \frac{\partial Q_{(u_i,k^i_d),(u_j,k^i_d)}}{\partial Q_{(v_x,k_m),(v_y,k_n)}} + \left[\mu^{im}_{u_i} P^{+}_{(u_i,k^i_e),(u_j,k^i_d)} + \Lambda^{t}_{u_i,k^i_d} Q_{(u_i,k^i_d),(u_j,k^i_d)} \right] \frac{\partial q_{u_i}}{\partial Q_{(v_x,k_m),(v_y,k_n)}} \right\} \tag{20}$$

$$\frac{\partial q_{u_m}}{\partial Q_{(v_x,k_m),(v_y,k_n)}} = \frac{1}{\mu^{ps}_{u_m} + \Lambda^{t}_{u_m,k^i_c} + \Lambda^{-}_{u_m,k^i_c}} * \sum_{j=1}^{N_{ps}} \left\{ \Lambda^{t}_{u_j,k^i_c} q_{u_j} \frac{\partial Q_{(u_j,k^i_c),(u_m,k^i_c)}}{\partial Q_{(v_x,k_m),(v_y,k_n)}} + \left[\mu^{ps}_{u_j} P^{+}_{(u_j,k^i_c),(u_m,k^i_c)} + \Lambda^{t}_{u_j,k^i_c} Q_{(u_j,k^i_c),(u_m,k^i_d)} \right] \frac{\partial q_{u_j}}{\partial Q_{(v_x,k_m),(v_y,k_n)}} \right\} \tag{21}$$

Since an arbitrary utilisation rate q_{l_i} of an entity (PoI or device) is determined by utilisation rate q_{l_j} of all the other entities, we can eliminate $\frac{\partial q_{l_i}}{\partial Q_{(v_x,k_m),(v_y,k_n)}}$ by representing equation (19), (20) and (21) in a matrix format. By defining $\mathbf{q_{l_i}}$ as a $N \times 1$ vector, $\mathbf{A_{en}} = diag(\frac{1}{\mu^{en}_{n_1} + \Lambda^{t}_{n_1,k^1_e}}, \ldots, \frac{1}{\mu^{en}_{n_{N_{en}}} + \Lambda^{t}_{n_{N_{en}},k^{N^c_{en}}_e}})$, $\mathbf{A_{im}} = diag(\frac{1}{\mu^{im}_{u_1} + \Lambda^{t}_{u_1,k^1_d} + \Lambda^{-}_{u_1,k^1_d}}, \ldots, \frac{1}{\mu^{im}_{u_1} + \Lambda^{t}_{u_{N_{im}},k^{N^c_{im}}_d} + \Lambda^{-}_{u_{N_{im}},k^{N^c_{im}}_d}})$, $\mathbf{A_{ps}} = diag(\frac{1}{\mu^{ps}_{u_1} + \Lambda^{t}_{u_1,k^1_c} + \Lambda^{-}_{u_1,k^1_c}}, \ldots, \frac{1}{\mu^{im}_{u_1} + \Lambda^{t}_{u_{N_{ps}},k^{N^c_{ps}}_c} + \Lambda^{-}_{u_{N_{ps}},k^{N^c_{ps}}_c}})$, $\mathbf{B_{en/im/ps}}$ as a $N \times N$ matrix whose elements are determined as follows in equation (23), $\mathbf{C_{en/im/ps}}$ as a $N \times N$ matrix with $\mathbf{C}(i,j) = \mu^{en/im/ps}_{l_j} P^{+}_{(l_j,k^i_{e/d/c}),(l_i,k^i_{e/d/c})}$, $\mathbf{D_{en/im/ps}}$ as a $N \times N$ matrix with $\mathbf{D}(i,j) = \Lambda^{t}_{l_j,k^i_{e/d/c}} Q_{(l_j,k^i_{e/d/c}),(l_i,k^i_{e/d/c})}$.

To determine the elements in matrix $\mathbf{B}$, we first need to determine the value of $\frac{\partial Q_{n_j,n_i}}{\partial Q_{(v_x,k_m),(v_y,k_n)}}$ by using relation $Q_{(v_x,k_m),(v_y,k_n)} = 1 - \sum_{k \neq y} Q_{n_x,n_k}$:

$$\frac{\partial Q_{(n_j,k_\psi),(n_i,k_\phi)}}{\partial Q_{(v_x,k_m),(v_y,k_n)}} = \begin{cases} 1, & \text{if } j = x,\ i = y, \psi = m, \phi = n \\ -1, & \text{if } j = x,\ i \neq y, \psi = m, \phi = n \\ 0, & \text{otherwise} \end{cases} \tag{22}$$

then matrix $\mathbf{B_{en/im/ps}}$ can be derived as:

$$\mathbf{B_{en/im/ps}}(i,j) = \begin{cases} \Lambda^{t}_{l_j,k^i_{e/d/c}}, & j = x, i = y, \psi = m, \phi = n \\ -\Lambda^{t}_{l_j,k^i_{e/d/c}}, & j = x, i \neq y, \psi = m, \phi = n \\ 0, & \text{otherwise} \end{cases} \tag{23}$$

Therefore, for an arbitrary PoI or device, $\frac{\partial \mathbf{q_{l_i}}}{\partial Q_{(v_x,k_m),(v_y,k_n)}}$ can be obtained as:

$$\frac{\partial \mathbf{q_{l_i}}}{\partial Q_{(v_x,k_m),(v_y,k_n)}} = \left[\mathbf{E_N} - \mathbf{A}(\mathbf{C}+\mathbf{D})\right]^{-1}\mathbf{ABq_n} \quad (24)$$

where term $\mathbf{E_N}$ is a $N \times N$ identity matrix.

Hence, the partial derivative of the overall goal function can be written as:

$$\begin{aligned}&\frac{\partial G}{\partial Q_{(v_x,k_m),(v_y,k_n)}} = \\ &\alpha \mathbf{F_{en}}\left[\mathbf{E_{N_{en}}} - \mathbf{A_{en}}(\mathbf{C_{en}}+\mathbf{D_{en}})\right]^{-1}\mathbf{A_{en}B_{en}q_{en}} \\ &+ \beta \mathbf{F_{im}}\left[\mathbf{E_{N_{im}}} - \mathbf{A_{im}}(\mathbf{C_{im}}+\mathbf{D_{im}})\right]^{-1}\mathbf{A_{im}B_{im}q_{im}} \\ &+ \gamma \mathbf{F_{ps}}\left[\mathbf{E_{N_{ps}}} - \mathbf{A_{ps}}(\mathbf{C_{ps}}+\mathbf{D_{ps}})\right]^{-1}\mathbf{A_{ps}B_{ps}q_{ps}}\end{aligned} \quad (25)$$

where term $\mathbf{F_{en/im/ps}}$ is a $1 \times N$ vector that can be derived from equation (15), (16), and (18) $\mathbf{F_{en}} = (\frac{1}{2}(N_{n_1} - O_{n_1}), \ldots, \frac{1}{2}(N_{n_{N_{en}}} - O_{n_{N_{en}}}))$, $\mathbf{F_{im}} = (\frac{1}{\Lambda^+_{u_1}}[\frac{q_{u_1}}{(1-q_{u_1})^2} + \frac{1}{1-q_{u_1}}], \ldots, \frac{1}{\Lambda^+_{u_{N_{im}}}}[\frac{q_{u_{N_{im}}}}{(1-q_{u_{N_{im}}})^2} + \frac{1}{1-q_{u_{N_{im}}}}])$, $\mathbf{F_{en}} = (N_{ps}(u_1)q_{u_1}^{N_{ps}(u_1)-1}, \ldots, N_{ps}(u_{N_{ps}})q_{u_{N_{ps}}}^{N_{ps}(u_{N_{ps}})-1})$.

The next step to solve equation (25) is to determine each q_{l_i}. Since each q_{l_i} is impacted by all the other linked q_{l_j} as shown in nonlinear equation (3), we determine the optimal value numerically with the procedures shown in Pseudocode 1. Finally, we compute $Q_{(v_x,k_m),(v_y,k_n)}$ using the following iterations:

Pseudocode 1 The procedures of solving q_{l_i}.

1: Set the initial value of q_{l_i} ($i = 1, \ldots, N$, N is the number of nodes in the network) to a random value between 0 and 1 (0 and 1 are excluded).
2: Solve q_{l_i} by substituting q_{l_j} ($j = 1, \ldots, N$, $j \neq i$) with their latest values. If the value of q_{l_j} is larger than 1, then reset it to 1.
3: Calculate q_{l_i} until $\left|q_{l_i}^{current} - q_{l_i}^{previous}\right| < c$, where $q_{l_i}^{current}$ is the current value of q_{l_i}, $q_{l_i}^{previous}$ is the previous value of q_{l_i}, and c is a certain threshold.

$$Q^{n+1}_{(n_j,k_\psi),(n_i,k_\phi)} = Q^{n}_{(n_j,k_\psi),(n_i,k_\phi)} - \eta \frac{\partial G}{\partial Q^{n}_{(n_j,k_\psi),(n_i,k_\phi)}} \quad (26)$$

where $\eta > 0$ is the learning rate.

V. Simulation Models and Assumptions

We employ the layout of the Xizhimen metro station in Beijing, China as the designated area as shown in Figure 6 We assume that there are 40 emergency lights, 3 on-site computers, and 51 sensors in the targeted area. We also assume that evacuees are equipped with smartphones that can perform local computation as well as information and energy exchange with other IoT devices. We also assume that a number of pavement locations are equipped with piezoelectric energy harvesters for energy collecting. Each device can act one or more roles in the routing of evacuee, information and energy flows.

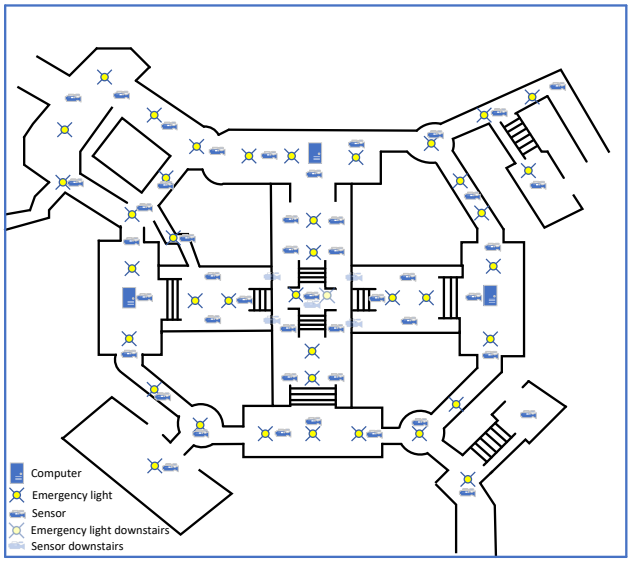

Fig. 6. The layout and deployment locations of transportation infrastructure entities of the metro station.

1) SS: sensors, smartphones;
2) EHD: piezoelectric energy harvesters, smartphones;
3) ES: smartphones, battery of sensors, battery of on-site computers, battery of emergency lights;
4) CD: smartphones, on-site computers;
5) AD: emergency lights, on-site computers.

The energy models for sensors, smartphones, wireless energy transfers, and piezoelectric energy harvester are reconstructed from [59], [60], [24] and [31], respectively and detailed models can be seen in Table I.

Besides our proposed algorithm, we also introduce two comparison algorithms to simulate the realistic behaviours of evacuees during emergency situations. The first one is called "normal egress algorithm", in which evacuees follow the static evacuation signs or routine paths to exits. When evacuees encounter obstacles in sight, they will revert to search alternative paths to exits. Since evacuees obtain no assistance from outside world, they can be trapped or consume plenty of time in finding other routes. This algorithm can be considered as a "static dijkstra's algorithm" and simulates the realistic evacuation processes in most of the current metro stations. The second comparison algorithm is called "Dijkstra's algorithm based algorithm". In this case, we assume that each evacuee is equipped with a portable device with a pre-installed route navigation application. The route navigation application can provide evacuees with the safest shortest paths (each edge is assigned with a "hazard intensity" which is a product of physical distance and hazard level.) to exits in a dynamic manner. This algorithm can be considered as a "dynamic dijkstra's algorithm" and can simulate the computer-aided evacuation processes.

Notation	Formula	Value
Sensors		
Energy consumption in sensing	$E_s^s B$	Term E_s^s is the energy consumed in sensing per bit and is chosen to be $5*10^{-8}$, term B is the number of bits in sensing, transmitting or receiving.
Energy consumption in information packet transmissions	$E_d^s B d^{\varepsilon} + E_t^s B$	Term E_d^s is the energy dissipated per bit per m^2 and is chosen to be $10 * 10^{-11}$, E_t^s is the energy consumed by transmission circuitry per bit and is chosen to be $5 * 10^{-8}$. Term d is the distance from transmitter to receiver. Term ε is a constant which depends on the attenuation the signal will suffer in the environment and is set to 2.
Energy consumption in information packet receptions	$E_r^s B$	Term e_l is the energy consumed by reception circuitry per bit and is chosen to be $5 * 10^{-8}$.
Energy consumption in idle state for a time interval of t	$E_{ci}^s t$	Term E_{ci}^s is the power of a sensor in idle state and is set to $9.6 * 10^{-3}$ watts.
Computers		
Energy consumption in active state for a time interval of t	$E_{ca}^c t$	Term E_{ca}^c is the power of a computer in active state and is set to 200 watts.
Energy consumption in idle state for a time interval of t	$E_{ci}^c t$	Term E_{ci}^c is the power of a computer in idle state and is set to 30 watts.
Smartphones		
Energy consumption in sending data to other devices	$E_t^p B$	Term E_t^P is the energy spent in sending data per bit and is chosen to be $4.21875 * 10^{-5}$.
Energy consumption in receiving data from other devices	$E_r^p B$	Term E_r^p is the energy spent in receiving data per bit and is chosen to be $1.53 * 10^{-4}$.
Energy consumption in active state for a time interval of t	$E_a^p t$	Term E_a^p is the energy spent in active state and is chosen to be 1.5 watts.
Energy consumption in idle state for a time interval of t	$E_i^p t$	Term E_i^p is the energy spent in idle state and is chosen to be 0.3 watts.
Battery capacity of smartphones	C_b^p	Term C_b^p stands for the battery capacity of smartphones and is chosen to be 40 kilojoules. The remaining energy of smartphones is set to be a random value.
Piezoelectric energy harvesters		
Output energy of Piezoelectric energy harvesters	$p_g^{peh} t$	Term p_g^{peh} is the output power of a piezoelectric energy harvester (1 square meter) and is chosen to be 4 watts/second.
Wireless energy transfers		
Output energy of wireless energy transfers	$p_g^{wet} t$	Term p_g^{wet} is the output power of a wireless energy transfer and is chosen to be 10 watts/second.
Emergency lights		
Energy consumption of emergency lights	$p_c^l t$	Term p_c^l is the power of the emergency lights and is set to 30 watts.
Battery capacity	C_b^l	Term C_b^l stands for the battery capacity of emergency lights and is chosen to be 200 kilojoules. The remaining energy of emergency lights is set to be a random value.

TABLE I. ENERGY MODELS OF VARIOUS DEVICES IN THE TARGETED TRANSPORTATION INFRASTRUCTURE SYSTEM.

VI. EXPERIMENTS AND DISCUSSIONS

We design a Python based program that functions as a client to dynamically interact with an open-source simulation platform, namely Simulation of Urban MObility (SUMO) [61], which can simulation pedestrian behaviours in a microscopic and continuous manner as shown in Figure 7. Evacuees are modelled based the embedded pedestrian model of SUMO. Devices are formulated with separated classes with independent computing, energy and communication models, and are displayed in the simulator with "traci.poi" interface in SUMO. Each device can be added to the GUI as a layer by using traci.poi.add command, and each device is associated with a class to manage its attributes. In our simulation, we generate a graph-based network with bidirectional lanes to mimic the fact that evacuees can travel freely on the routes, yet we can also use traci.person.movetoXY command to mimic the free movement of evacuees in the whole space. Whenever detecting an entity arrives a PoI by examining the current (x, y) coordinates of the entity, different actions can be triggered and performed as such changing its current route.

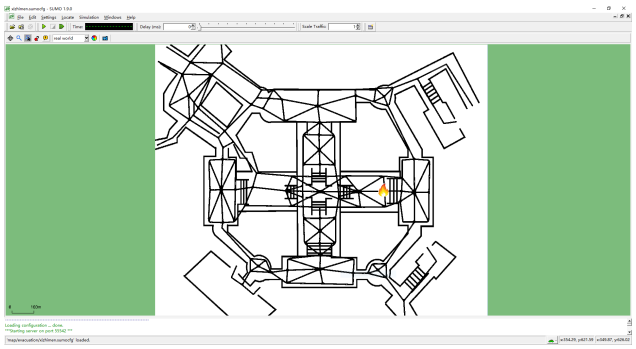

Fig. 7. The graphical user interface of the SUMO-based simulator.

To evaluate the effectiveness of our proposed algorithm, we designs two scenarios to mimic the common emergency events. The first scenario is a fire related disaster, in which evacuees need to egress to exits as soon as possible. The initial fire location is shown in Figure 7. The second one is an earthquake(power outage) related disaster, in which trapped evacuees need to avoid possible hazardous areas and evacuate to safe areas in a gentle fashion. We also utilise the static evacuation algorithm and Dijkstra's aided evacuation algorithm mentioned above for comparison purposes.

We assume that there are 6000 evacuees in the metro station when the disaster breaks out. The evacuees are randomly scattered within the target metro stations in 10 simulation runs and the average values of the performance metrics are presented. The clearance time of the metro station in the first scenario is shown in Figure 8. As can be seen clearly, our proposed algorithm achieves the best performance among the three algorithms. This is mainly due to the dynamic distribution of pedestrians among possible PoIs by the introduction of $Q_{(u_i,k_c^i),(u_j,k_c^i)}$. By doing this, the "space" resource is being more sufficient used and congestion can be eased. The Dijkstra's algorithm is efficient in the early stage of the evacuation

process but can cause severe congestion on the shortest path owing to the accumulated concentration of evacuees. This can also be verified by the survival rates of the three algorithm in the first scenario, as shown in Figure 10. The distributions of pedestrian flows of the three algorithms are displayed in Figure 11 to 13, as can be seen clearly, the balancing of flow ratios at each PoI when using G-network based algorithm can make more sufficient use of the "space" resource. Similarly, Figure 14 and 15 shows the effectiveness of the algorithm in balancing and allocating the resources in information and energy flows. The impact of the energy replenishment algorithm (energy flow optimisation) is shown in Figure 16, the main energy sources are the piezoelectric energy harvesters and the wireless energy transfers while the main energy cosumers are emergency light, computers, sensors, smartphones, losses in wireless energy transfers, etc. As can be seen in the figure, although the proposed algorithm consume the most energy in the three algorithms, it also generate and collect the most energy owing the more visits of the piezoelectric energy harvesters as well as the introduction of the energy replenishment algorithm.

The average service delays of the emergency requests in the first scenario are shown in Figure 9. This metric is calculated every 100 seconds with respect to the queue length of the emergency requests to the computers. The G-network aided approach actually suffers from higher service delay at the start of the evacuation process in comparison with the Dijkstra's algorithm, this is mainly because the G-network aided approach needs to optimise not only pedestrian flows but also information and energy flows. However, with the fast clearance of evacuees, the computation workload of the G-network aided approach drops remarkably.

In the second scenario, we assume that evacuees are trapped in the metro station and may need to dynamically change their positions to avoid possible hazards. The survival rates in this situation are shown in Figure 17. The G-network aided approach performs the best since it can make more efficient use of the system resources to maintain the service continuity of the ERS. Hence, evacuees can dynamically receive emergency instructions to avoid hazards. On the other hand, since the Dijkstra's algorithm does not introduce energy flow optimisation, the heavy communications and computations of the system can quickly drain the energy storages and cause the malfunction of the system. This can also be proved by Figure 18. As the G-network aided approach can achieve much longer service time. This is mainly caused by the introduction of energy harvesting techniques and the energy flow optimisation among IoT devices.

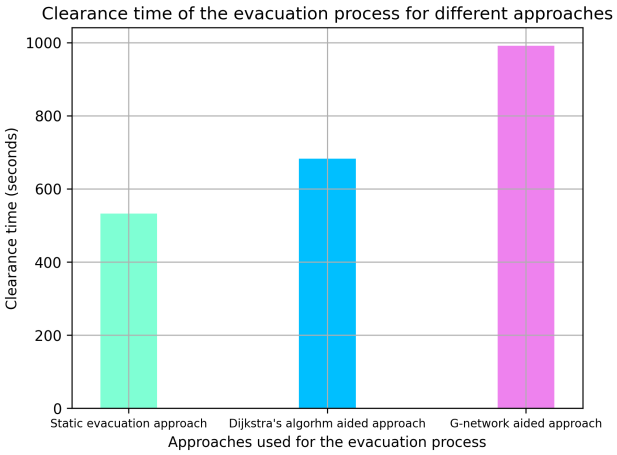

Fig. 8. The clearance times of the evacuation process for different approaches in the first scenario. "Static evacuation approach" represents the use of static evacuation signs or routine paths, and without the assistance of ERS. "Dijkstra's algorhm aided approach" uses the classical Dijkstra's algorithm for evacuation route planning. "G-network aided approach" stands for our proposed algorithm.

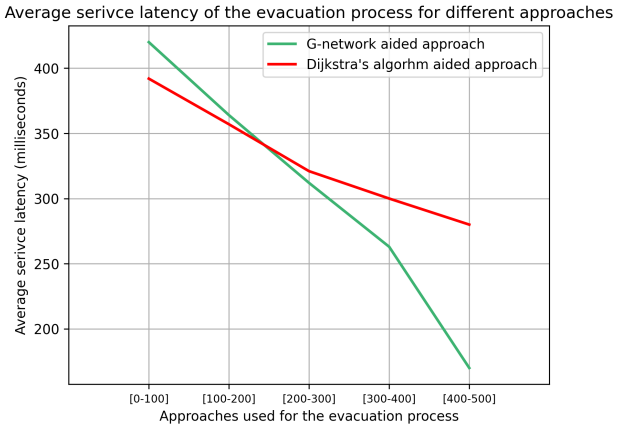

Fig. 9. The average service latencies of the evacuation process for different approaches in the first scenario. The average service latency is calculated every 100 seconds.

VII. Conclusions

The effectiveness of the modern transportation infrastructure systems such as emergency response systems can significantly protect victims from the first strike of hazards. It therefore prolongs the duration of an evacuation process and highlights the importance of service continuity of emergency response systems under the threat of power outage. In this paper, we proposes a G-network based queueing network model to mimic the interactive behaviours among different infrastructures and devices. The directions of flows of pedestrians, information and energy are optimised by making use of the product form solution of the G-network model and calculated with a gradient decent algorithm. Furthermore, we improve the power supply resilience of the emergency response system by using energy collected by piezoelectric energy harvesters and exchanged by wired cables or wireless energy transfers. Future research will be directed to the use of big data analysis [62] to better reflect the behaviours of evacuees during emergency situations and the introduction of Electroencephalogram (EEG) aided deep learning techniques [63], [64], [65] to better evaluate the quality of experience of evacuees.

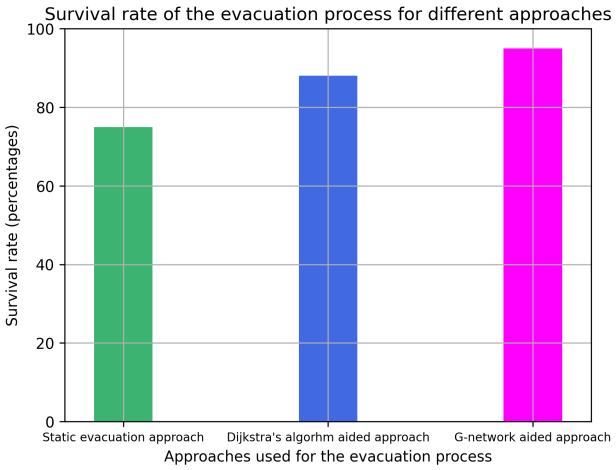

Fig. 10. The survival rates of the evacuation process for different approaches in the first scenario.

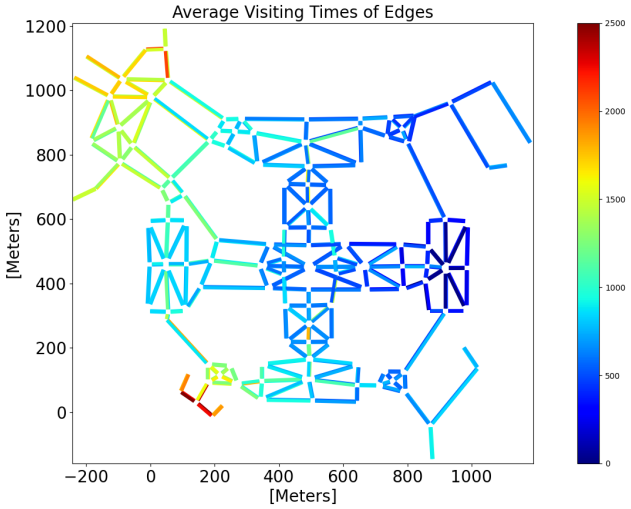

Fig. 11. The average visiting times of evacuees on each edge while using static evacuation algorithm.

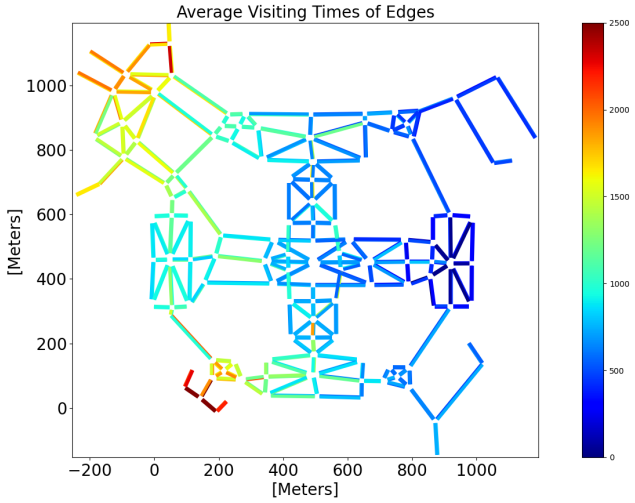

Fig. 12. The average visiting times of evacuees on each edge while using Dijkstra based evacuation algorithm.

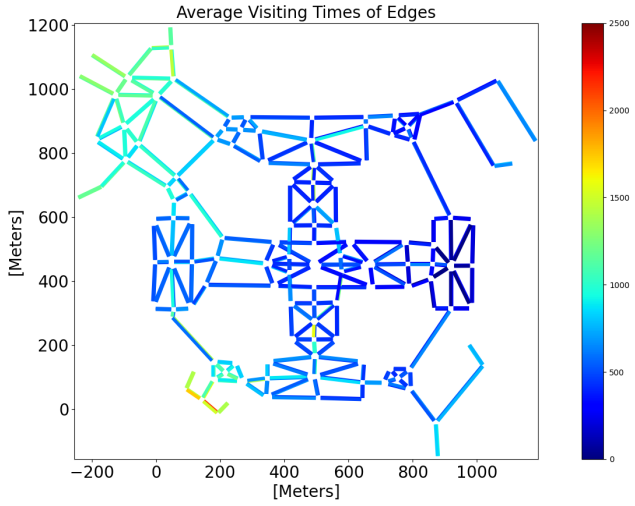

Fig. 13. The average visiting times of evacuees on each edge while using G-network based evacuation algorithm.

ACKNOWLEDGMENT

This work is funded in part by the Beijing Natural Science Foundation Program (Grant No. 21L00097), and International Research Cooperation Seed Fund of Beijing University of Technology (Grant No. 2021A04 and 2021B14) and Postdoctoral Research Foundation of China (Grant No. 2021M690341).

REFERENCES

[1] J. Wang, C. Jiang, H. Zhang, Y. Ren, K.-C. Chen, and L. Hanzo, "Thirty years of machine learning: The road to pareto-optimal wireless networks," *IEEE Communications Surveys Tutorials*, vol. 22, no. 3, pp. 1472–1514, 2020.

[2] J. Wang, C. Jiang, K. Zhang, T. Q. S. Quek, Y. Ren, and L. Hanzo, "Vehicular sensing networks in a smart city: Principles, technologies and applications," *IEEE Wireless Communications*, vol. 25, no. 1, pp. 122–132, 2018.

[3] H. Bi and E. Gelenbe, "A survey of algorithms and systems for evacuating people in confined spaces," *Electronics*, vol. 8, no. 6, p. 711, 2019.

[4] N. A. Pantazis, S. A. Nikolidakis, and D. D. Vergados, "Energy-efficient routing protocols in wireless sensor networks: A survey," *IEEE Communications surveys & tutorials*, vol. 15, no. 2, pp. 551–591, 2012.

[5] D. Feng, C. Jiang, G. Lim, L. J. Cimini, G. Feng, and G. Y. Li, "A survey of energy-efficient wireless communications," *IEEE Communications Surveys & Tutorials*, vol. 15, no. 1, pp. 167–178, 2012.

[6] J. Wang, C. Jiang, K. Zhang, X. Hou, Y. Ren, and Y. Qian, "Distributed q-learning aided heterogeneous network association for energy-efficient iiot," *IEEE Transactions on Industrial Informatics*, vol. 16, no. 4, pp. 2756–2764, 2019.

[7] L. Xu, R. Collier, and G. M. O'Hare, "A survey of clustering techniques in wsns and consideration of the challenges of applying such to 5g iot scenarios," *IEEE Internet of Things Journal*, vol. 4, no. 5, pp. 1229–1249, 2017.

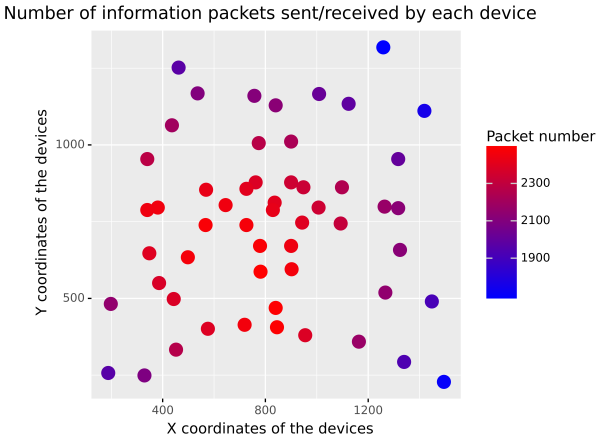

Fig. 14. The average number times of information packets sent/received by devices while using G-network based evacuation algorithm.

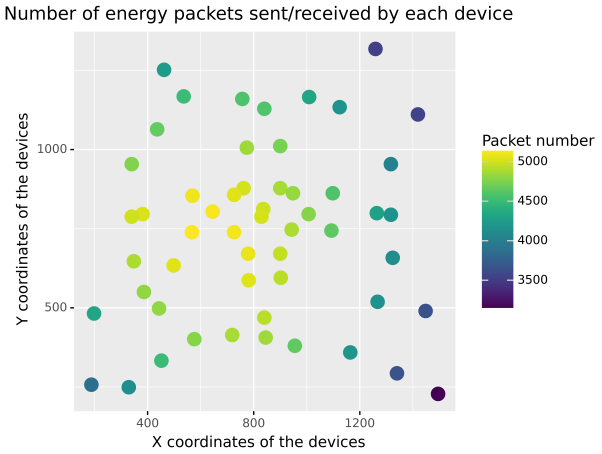

Fig. 15. The average number times of energy packets sent/received by devices while using G-network based evacuation algorithm.

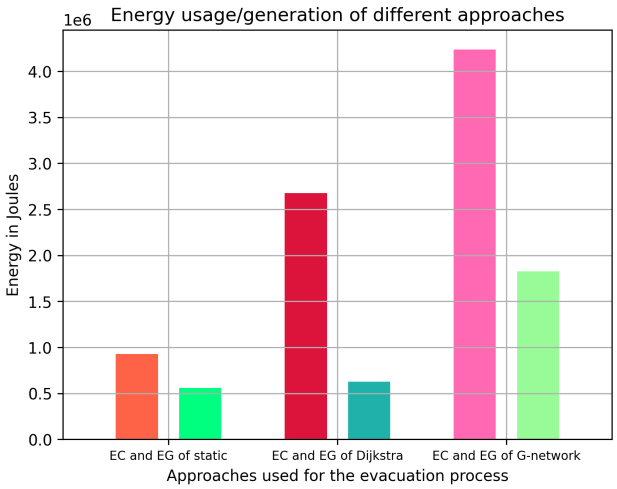

Fig. 16. The energy consumption (EC) and energy generation (EG) in a 5-minutes evacuation process for different approaches in the first scenario. The energy harvested by wireless energy transfers has been counted in the last algorithm.

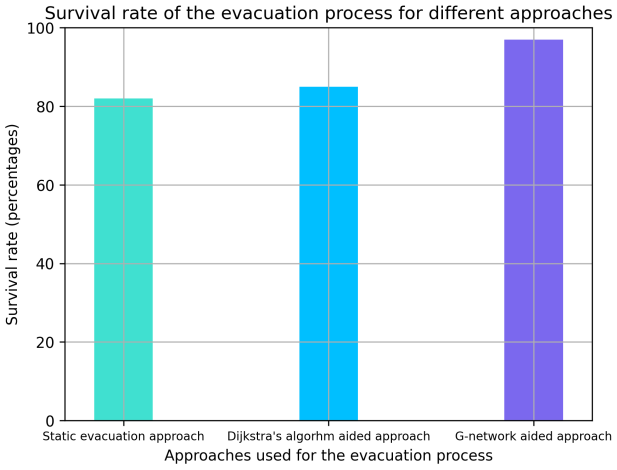

Fig. 17. The survival rates of the evacuation process for different approaches in the second scenario.

[8] V. Rodoplu and T. H. Meng, "Bits-per-joule capacity of energy-limited wireless networks," *IEEE Transactions on Wireless Communications*, vol. 6, no. 3, pp. 857–865, 2007.

[9] C. Van Phan, Y. Park, H. H. Choi, J. Cho, and J. G. Kim, "An energy-efficient transmission strategy for wireless sensor networks," *IEEE Transactions on Consumer Electronics*, vol. 56, no. 2, pp. 597–605, 2010.

[10] D. Ye and M. Zhang, "A self-adaptive sleep/wake-up scheduling approach for wireless sensor networks," *IEEE transactions on cybernetics*, vol. 48, no. 3, pp. 979–992, 2017.

[11] L. Song, K. K. Chai, Y. Chen, J. Schormans, J. Loo, and A. Vinel, "Qos-aware energy-efficient cooperative scheme for cluster-based iot systems," *IEEE Systems Journal*, vol. 11, no. 3, pp. 1447–1455, 2017.

[12] E. Gelenbe, "Steps toward self-aware networks," *Communications of the ACM*, vol. 52, no. 7, pp. 66–75, 2009.

[13] S. Ezdiani, I. S. Acharyya, S. Sivakumar, and A. Al-Anbuky, "Wireless sensor network softwarization: Towards wsn adaptive qos," *IEEE Internet of Things Journal*, vol. 4, no. 5, pp. 1517–1527, 2017.

[14] T. Lv, Z. Lin, P. Huang, and J. Zeng, "Optimization of the energy-efficient relay-based massive iot network," *IEEE Internet of Things Journal*, vol. 5, no. 4, pp. 3043–3058, 2018.

[15] B. Omoniwa, R. Hussain, M. Adil, A. Shakeel, A. K. Tahir, Q. U. Hasan, and S. A. Malik, "An optimal relay scheme for outage minimization in fog-based internet-of-things (iot) networks," *IEEE Internet of Things Journal*, vol. 6, no. 2, pp. 3044–3054, 2018.

[16] S. Albers, "Energy-efficient algorithms," *Communications of the ACM*, vol. 53, no. 5, pp. 86–96, 2010.

[17] O. B. Akan, O. Cetinkaya, C. Koca, and M. Ozger, "Internet of hybrid energy harvesting things," *IEEE Internet of Things Journal*, vol. 5, no. 2, pp. 736–746, 2017.

[18] Z. Hou, H. Chen, Y. Li, and B. Vucetic, "Incentive mechanism design for wireless energy harvesting-based internet of things," *IEEE Internet of Things Journal*, vol. 5, no. 4, pp. 2620–2632, 2017.

[19] H. Ko, S. Pack, and V. C. Leung, "Spatiotemporal correlation-based environmental monitoring system in energy harvesting internet of things (iot)," *IEEE Transactions on Industrial Informatics*, vol. 15, no. 5, pp. 2958–2968, 2018.

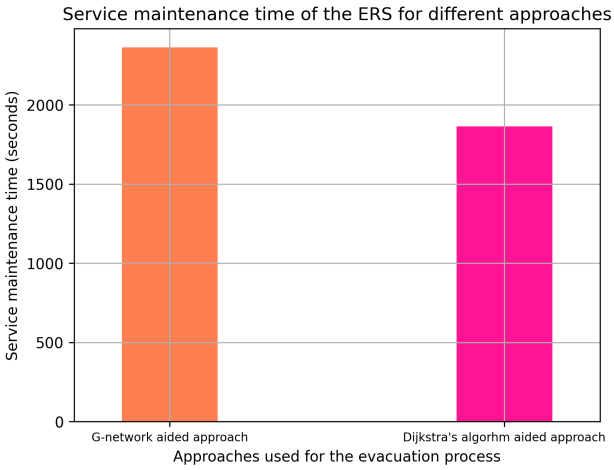

Fig. 18. The service maintenance time of the evacuation process for different approaches. The service maintenance time is defined as the time duration before the power outage of the first on-site computer.

[20] L. Guo, Z. Chen, D. Zhang, J. Liu, and J. Pan, "Sustainability in body sensor networks with transmission scheduling and energy harvesting," *IEEE Internet of Things Journal*, vol. 6, no. 6, pp. 9633–9644, 2019.

[21] X. Chen, W. Ni, X. Wang, and Y. Sun, "Optimal quality-of-service scheduling for energy-harvesting powered wireless communications," *IEEE Transactions on Wireless Communications*, vol. 15, no. 5, pp. 3269–3280, 2016.

[22] X. Huang, R. Yu, J. Kang, Z. Xia, and Y. Zhang, "Software defined networking for energy harvesting internet of things," *IEEE Internet of Things Journal*, vol. 5, no. 3, pp. 1389–1399, 2018.

[23] D. Minoli, K. Sohraby, and B. Occhiogrosso, "Iot considerations, requirements, and architectures for smart buildings—energy optimization and next-generation building management systems," *IEEE Internet of Things Journal*, vol. 4, no. 1, pp. 269–283, 2017.

[24] W. Xu, W. Liang, J. Peng, Y. Liu, and Y. Wang, "Maximizing charging satisfaction of smartphone users via wireless energy transfer," *IEEE Transactions on Mobile Computing*, vol. 16, no. 4, pp. 990–1004, 2016.

[25] S. Cao, "The impact of electric vehicles and mobile boundary expansions on the realization of zero-emission office buildings," *Applied Energy*, vol. 251, p. 113347, 2019.

[26] N. Gray, S. McDonagh, R. O'Shea, B. Smyth, and J. D. Murphy, "Decarbonising ships, planes and trucks: An analysis of suitable low-carbon fuels for the maritime, aviation and haulage sectors," *Advances in Applied Energy*, vol. 1, p. 100008, 2021.

[27] H. Pan, L. Qi, Z. Zhang, and J. Yan, "Kinetic energy harvesting technologies for applications in land transportation: A comprehensive review," *Applied Energy*, vol. 286, p. 116518, 2021.

[28] G. Lan, W. Xu, D. Ma, S. Khalifa, M. Hassan, and W. Hu, "Entrans: Leveraging kinetic energy harvesting signal for transportation mode detection," *IEEE Transactions on Intelligent Transportation Systems*, vol. 21, no. 7, pp. 2816–2827, 2019.

[29] M. Gao, P. Wang, Y. Cao, R. Chen, and D. Cai, "Design and verification of a rail-borne energy harvester for powering wireless sensor networks in the railway industry," *IEEE Transactions on Intelligent Transportation Systems*, vol. 18, no. 6, pp. 1596–1609, 2016.

[30] H. Xiong and L. Wang, "Piezoelectric energy harvester for public roadway: On-site installation and evaluation," *Applied Energy*, vol. 174, pp. 101–107, 2016.

[31] G. J. Song, J. Y. Cho, K.-B. Kim, J. H. Ahn, Y. Song, W. Hwang, S. Do Hong, and T. H. Sung, "Development of a pavement block piezoelectric energy harvester for self-powered walkway applications," *Applied Energy*, vol. 256, p. 113916, 2019.

[32] J. Feng, Z. Ye, C. Wang, M. Xu, and S. Labi, "An integrated optimization model for energy saving in metro operations," *IEEE Transactions on Intelligent Transportation Systems*, vol. 20, no. 8, pp. 3059–3069, 2018.

[33] S. Heydari, P. Fajri, M. Rasheduzzaman, and R. Sabzehgar, "Maximizing regenerative braking energy recovery of electric vehicles through dynamic low-speed cutoff point detection," *IEEE Transactions on Transportation Electrification*, vol. 5, no. 1, pp. 262–270, 2019.

[34] E. Gelenbe and A. Labed, "G-networks with multiple classes of signals and positive customers," *European journal of operational research*, vol. 108, no. 2, pp. 293–305, 1998.

[35] E. Gelenbe and H. Bi, "Emergency navigation without an infrastructure," *Sensors*, vol. 14, no. 8, pp. 15 142–15 162, 2014. [Online]. Available: http://www.mdpi.com/1424-8220/14/8/15142

[36] H. Bi, Y. Chen, W.-L. Shang, C. Song, and W. Huang, "Self-administered information sharing framework using bioinspired mechanisms," *Complexity*, vol. 2020, 2020.

[37] M. Qiu, Z. Ming, J. Wang, L. T. Yang, and Y. Xiang, "Enabling cloud computing in emergency management systems," *IEEE Cloud Computing*, vol. 1, no. 4, pp. 60–67, 2014.

[38] H. Bi and E. Gelenbe, "Routing diverse evacuees with cognitive packets," in *Pervasive Computing and Communications Workshops (PERCOM Workshops), 2014 IEEE International Conference on*, March 2014, pp. 291–296.

[39] E. Gelenbe and Z. Kazhmaganbetova, "Cognitive packet network for bilateral asymmetric connections," *IEEE Transactions on Industrial Informatics*, vol. 10, no. 3, pp. 1717–1725, 2014.

[40] H. Bi and O. H. Abdelrahman, "Energy-aware navigation in large-scale evacuation using g-networks," *Probability in the Engineering and Informational Sciences*, vol. 32, no. 3, pp. 340–352, 2018.

[41] J.-H. Liao and D. Shaw, "The use of laser scattering and energy harvesting technology for fire evacuation," *Safety science*, vol. 55, pp. 165–172, 2013.

[42] H. Bi, W.-L. Shang, and Y. Chen, "Cooperative and energy-efficient strategies in emergency navigation using edge computing," *IEEE Access*, vol. 8, pp. 54 441–54 455, 2020.

[43] E. Gelenbe and Y. Zhang, "Performance optimization with energy packets," *IEEE Systems Journal*, vol. 13, no. 4, pp. 3770–3780, 2019.

[44] Y. M. Kadioglu and E. Gelenbe, "Product-form solution for cascade networks with intermittent energy," *IEEE Systems Journal*, vol. 13, no. 1, pp. 918–927, 2018.

[45] F. Yang and M. Wang, "A review of systematic evaluation and improvement in the big data environment," *Frontiers of Engineering Management*, vol. 7, no. 1, pp. 27–46, 2020.

[46] E. Gelenbe, "The first decade of g-networks," *European Journal of Operational Research*, vol. 126, no. 2, pp. 231–232, 2000. [Online]. Available: http://dx.doi.org/10.1016/S0377-2217(99)00475-0

[47] E. Gelenbe, "Product-form queueing networks with negative and positive customers," *Journal of Applied Probability*, pp. 656–663, 1991.

[48] E. Gelenbe, "G-networks with signals and batch removal," *Probability in the Engineering and Informational Sciences*, vol. 7, no. 3, pp. 335–342, 1993.

[49] E. Gelenbe, "G-networks with triggered customer movement," *Journal of Applied Probability*, pp. 742–748, 1993.

[50] E. Gelenbe and J.-M. Fourneau, "G-networks with resets," *Performance Evaluation*, vol. 49, no. 1, pp. 179–191, 2002.

[51] R. O. Onvural, *Asynchronous transfer mode networks: performance issues*. Artech House, Inc., 1995.

[52] E. Gelenbe and G. Pujolle, "Introduction to networks of queues," *John Wiley Ltd, New York and Chichester*, 1998.

[53] E. Gelenbe and C. Morfopoulou, "A framework for energy-aware

routing in packet networks," *The Computer Journal*, vol. 54, no. 6, pp. 850–859, 2011.

[54] E. Gelenbe, "Energy packet networks: adaptive energy management for the cloud," in *Proceedings of the 2nd International Workshop on Cloud Computing Platforms*. ACM, 2012, p. 1.

[55] E. Gelenbe, "Energy packet networks: smart electricity storage to meet surges in demand," in *Proceedings of the 5th International ICST Conference on Simulation Tools and Techniques*. ICST (Institute for Computer Sciences, Social-Informatics and Telecommunications Engineering), 2012, pp. 1–7.

[56] E. Gelenbe, "Dealing with software viruses: a biological paradigm," *Information Security Technical Report*, vol. 12, no. 4, pp. 242–250, 2007.

[57] E. Gelenbe, "Steady-state solution of probabilistic gene regulatory networks," *Physical Review E*, vol. 76, no. 3, p. 31903, 2007.

[58] E. Gelenbe and E. T. Ceran, "Energy packet networks with energy harvesting," *Ieee Access*, vol. 4, pp. 1321–1331, 2016.

[59] E. J. Duarte-Melo and M. Liu, "Analysis of energy consumption and lifetime of heterogeneous wireless sensor networks," in *Global Telecommunications Conference, 2002. GLOBECOM'02. IEEE*, vol. 1. IEEE, 2002, pp. 21–25.

[60] A. Carroll and G. Heiser, "An analysis of power consumption in a smartphone," in *Proceedings of the 2010 USENIX conference on USENIX annual technical conference*, 2010, pp. 21–21.

[61] M. Behrisch, L. Bieker, J. Erdmann, and D. Krajzewicz, "Sumo–simulation of urban mobility," in *The Third International Conference on Advances in System Simulation (SIMUL 2011), Barcelona, Spain*, vol. 42, 2011.

[62] W.-L. Shang, J. Chen, H. Bi, Y. Sui, Y. Chen, and H. Yu, "Impacts of covid-19 pandemic on user behaviors and environmental benefits of bike sharing: A big-data analysis," *Applied Energy*, vol. 285, p. 116429, 2021.

[63] X. Tao, Z. Chen, M. Xu, and J. Lu, "Rebuffering optimization for dash via pricing and eeg-based qoe modeling," *IEEE Journal on Selected Areas in Communications*, vol. 37, no. 7, pp. 1549–1565, 2019.

[64] Y. Duan, Z. Li, X. Tao, Q. Li, S. Hu, and J. Lu, "Eeg-based maritime object detection for iot-driven surveillance systems in smart ocean," *IEEE Internet of Things Journal*, vol. 7, no. 10, pp. 9678–9687, 2020.

[65] S. Hu, Y. Duan, X. Tao, G. Ye Li, and J. Lu, "Brain-inspired image quality assessment method based on electroencephalography feature learning," in *2021 IEEE Global Communications Conference (GLOBECOM)*, 2021, pp. 1–6.

Huibo Bi received the B.Eng. and M.Eng. degrees from the Qingdao University of Science and Technology, China, in 2009 and Chongqing University, China, in 2012, respectively, and the Ph.D. degree in electrical and electronic engineering from Imperial College London in 2017, under the supervision of Prof. Erol Gelenbe. He is now a lecturer with the College of Metropolitan Transportation, Beijing University of Technology. His research interests include intelligent-networked systems, sensor networks, emergency management and distributed computing.

Wen-Long Shang is a Lecturer at the College of Metropolitan Transportation, Beijing University of Technology. Prior to joining Beijing University of Technology, he received his PhD degree from Centre for Transport Studies in Department of Civil and Environmental Engineering of Imperial College London. He has already published several academic papers in peer-reviewed journals and conferences. His research interests include but not limit to: analysis and processing of urban road network data, complex network theory, robustness and resilience of urban road networks, intelligent transport systems, safety science and smart city, large scale optimization and so on.

Yanyan Chen received the Ph.D. degree in Civil Engineering from Harbin University of technology, China, in 1997. Since 1999, she has worked at Beijing University of Technology and now is the dean of College of Metropolitan Transportation. Her research interests include urban transport planning, travel demand management policies, transport system reliability and big data mining. Professor Chen is a co-chair of urban transportation committee in China Highway & Transportation Society. She has published more than 100 articles in journals and 6 academic books.

Kezhi Wang received his B.E. and M.E. degrees in College of Automation from Chongqing University, China, in 2008 and 2011, respectively. He received his Ph.D. degree in Engineering from the University of Warwick, U.K. in 2015. He was a senior research officer in University of Essex, U.K. Currently he is a Senior Lecturer in Department of Computer and Information Sciences at Northumbria University, U.K. His research interests include wireless communication and mobile edge computing.